Eur Biophys J (1990) 17:325–329

European Biophysics Journal

SAXS study of the snake toxin α-crotamine

J. R. Beltran [1], Y. P. Mascarenhas [2,*], A. F. Craievich [3], and C. J. Laure [4]

[1] Instituto de Biociências, Letras e Ciências Exatas, UNESP, Departamento de Física, Caixa Postal 136-15055 São José do Rio Preto-SP, Brazil
[2] Instituto de Física e Química de São Carlos, Universidade de São Paulo, Caixa Postal 369-13560, São Carlos-SP, Brazil
[3] Laboratório Nacional de Luz Síncrotron/CNPq, Caixa Postal 6192-13081, Campinas-SP, and IFUSP, São Paulo, Brazil
[4] Faculdade de Medicina de Ribeirão Preto, Departamento de Bioquímica, Ribeirão Preto-SP-14100, Brazil

Received April 17, 1989/Accepted in revised form October 5, 1989

Abstract. α-crotamine is a small toxic protein (42 amino acid residues with three disulphide bridges) present in the venom of Crotallus durissus terrificus. Molecular parameters ($R_g = 13.7$ Å, $S = 3{,}000$ Å^2, $V = 9{,}200$ Å^3 and $D_{max} = 40$ Å) were derived from SAXS curves obtained from a solution of this protein at pH = 4.5. An excellent agreement between the experimental distance distribution curve and that calculated from a model consisting of two lobes linked by the Cys(18)-Cys(30) disulphide bridge.

Key words: Snake toxin, α-crotamine, small angle X-ray scattering, model for solution structure

1. Introduction

α-Crotamine is a neurotoxin often found in the crude venom of the Brazilian snake Crotallus durissus terrificus. It is a strongly basic polypeptide toxin, with a molecular weight of 4,870. It contains a total of 42 residues, of which six are half-cystines. It has a very high lysine (nine residues) and low arginine (two residues) content. The NH_2-terminus is tyrosine and the COOH-terminus glycine. α-crotamine has been sequenced by Laure (1975), who also located the three cystine bridges (Conti et al. 1980). The primary structure of α-crotamine with an indication of the position of the disulphide bridges is given in Fig. 1.

Raman studies by Kawano et al. (1982) suggested the presence of both β-structure and α-helix in α-crotamine, with the former predominating. Using polarimetric titration methods, Hampe et al. (1976) concluded that α-crotamine undergoes conformational changes with changes in pH. Beltran et al. (1985) confirmed these findings using SAXS and also obtained clear indications that α-crotamine may assume different aggregation states with changes in pH. For this work, it was possible to obtain fresh samples of α-crotamine that yielded monodisperse solutions at pH = 4.5.

2. Materials and methods

2.1. Preparation of the samples

The α-crotamine used in the experiments was obtained from the crude snake venom according to the following procedure: – The crude venom was filtered through a 4 × 45 cm Sephadex G-75 column using ammonium formate 0.05 M, pH = 3.5, buffer at a flow rate of 0.8 ml/min. Figure 2 shows that four or five chromatographic peaks are obtained (depending on the origin of the crotamine positive venom) with crotamine present in peak D. Peak D was then filtered on a similar column, allowing the separation of a contaminant from peak C, and then chromatographed on a 2 × 45 cm SP-Sephadex G-25 column using 0.84 M ammonium formate, pH = 3.5, buffer at a flow rate of 0.4 ml/min. Figure 3 shows that five peaks are obtained and these are named alpha, beta, gamma, delta and omega. The fraction corresponding to the α-peak

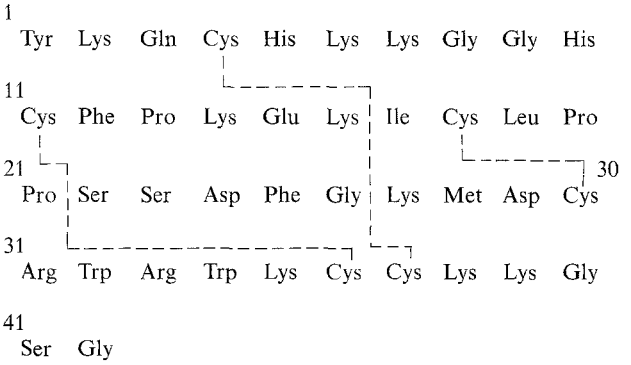

Fig. 1. Primary structure of α-crotamine with indication of the position of the disulphide bridges

* To whom offprint requests should be sent

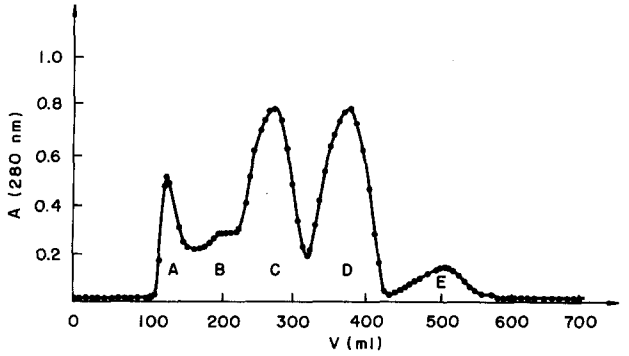

Fig 2. Chromatographic peaks obtained from crude crotamine positive venom of Crotallus durissus terrificus when filtered through a Sephadex G-75 column

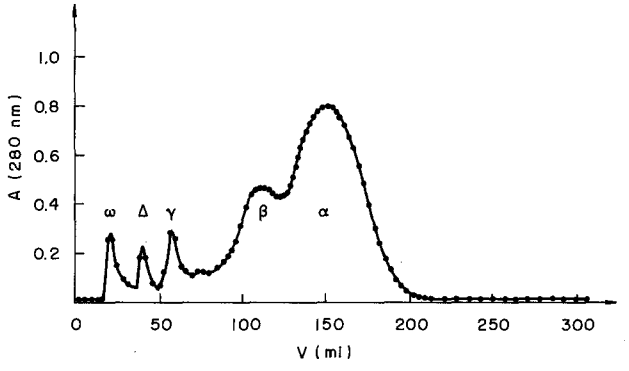

Fig. 3. Chromatographic peaks obtained from the crotamine peak when chromatographed on a SP-Sephadex G-25 column

was desalted by extensive dialysis, lyophilized and chromatographed on a similar column to yield a sample of pure α-crotamine.

The highest concentration sample used in the experiment was prepared by the addition of the appropriate amount of α-crotamine and solvent (HCl solutions at pH = 4.5). The same sample was further diluted to obtain the solutions at lower concentrations.

2.2 SAXS measurements

The protein solutions were placed in Lindemann glass capillary tubes of 1.0 mm diameter and kept at 22 C. The SAXS measurements were performed with CuKa filtered radiation. The experimental set-up consisted of a Kratky collimation system providing a beam of linear cross section (height: 44 mm and negligible width), an evacuated X-ray scattering path and a position-sensitive detector at 333 mm from the sample. The scattering intensities due to the solvent and capillary tube were subtracted from the total measured intensity and normalized to equivalent sample absorption and concentration. These experimental SAXS curves, $J(s)$, were determined as functions of the modulus of the scattering vector, s, defined by $s = 2\sin(\varepsilon/2)/\lambda$, ε being the scattering angle and λ the X-ray wavelength, for several protein concentrations. The SAXS measurements were carried out for an s domain ranging from 2.10^{-3} Å^{-1} up to 60.10^{-3} Å^{-1}. The intensity curves, $J(s)$, were desmeared for the beam linear cross section shape. The various desmeared curves, $I(s)$, were then extrapolated to zero concentration in order to eliminate concentration effects. The extrapolated function was used for the calculation of the distance distribution function. The experimental SAXS curves were smoothed to facilitate the extrapolation procedure.

2.3. Prediction of secondary structures

Denaturation-renaturation experiments on proteins have provided experimental evidence that the nature and sequence of amino acids are the main factors responsible for the very special folding of the polypeptide chain that gives rise to the secondary and tertiary structures of a protein. A whole series of methods that attempt to predict the secondary structure of a protein on the basis of the information contained in the primary structure have been devised. Two of them, that have proved to give a reliability of prediction on the order of 60%, were used to predict the secondary structure of α-crotamine. These are the Chou and Fasman (1977, 1978) method and the method of hydrophobicity profiles (Cid et al. 1982).

2.4. Computer programs

SAXS data were desmeared using the Glatter (1982) ITP program. This program was also used for the calculation of the distance distribution function, $p(r)$. The theoretical distance distribution function was calculated using the Glatter (1980) Multibody program.

3. Results and discussion

3.1. Scattering curves and molecular parameters

Guinier plots ($\log I(s)$ versus s^2) for α-crotamine solutions of 13, 12, 10.5, 8.5 and 7 weight % concentration, are given in Fig. 4. The apparent radii of gyration, R'_g, were determined from the slope, γ, of the linear region of $\log I$ versus s^2 plots as follows (Guinier and Fournet 1955):

$$R'_g = 0.418\sqrt{-\gamma} \qquad (1)$$

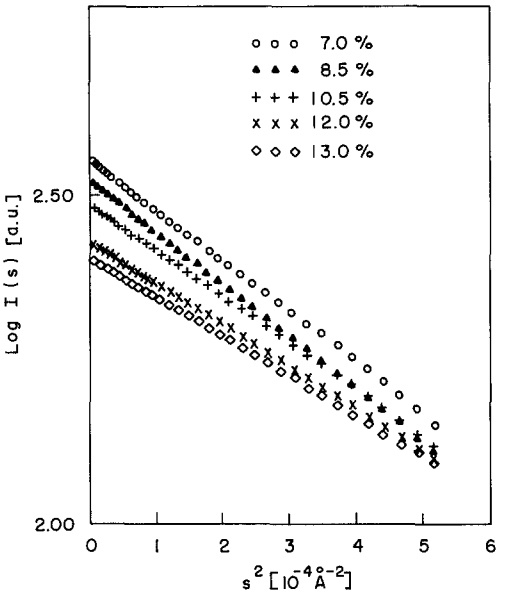

Fig. 4. Guinier plots ($\log I(s)$ versus s^2) for α-crotamine solutions of 13, 12, 10.5, 8.5 and 7 weight %

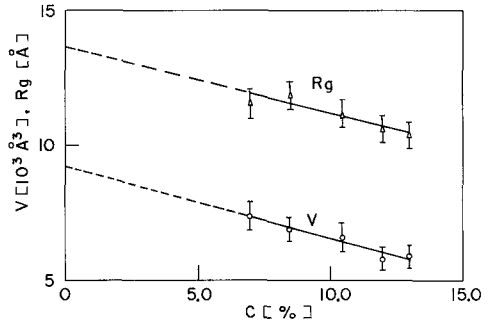

Fig. 5. R'_g and V' extrapolation to zero concentration for α-crotamine solutions, yielding $R_g = 13.7$ Å and $V = 9{,}200$ Å^3

Table 1. Molecular dimensions of α-crotamine

Conc. (mg/ml)	R_g (Å)	V (Å$^3 \times 10^3$)	S (Å$^2 \times 10^3$)
130	10.4±0.5	5.9±0.5	2.6±0.3
120	10.6±0.5	5.8±0.5	2.6±0.3
105	11.2±0.7	6.6±0.6	3.1±0.4
85	11.9±0.6	6.9±0.4	3.1±0.3
70	11.7±0.5	7.4±0.5	3.4±0.4
0	13.7±0.6	9.2±0.5	$\bar{s}$=3.0±0.3

The R'_g value has been plotted as a function of concentration in Fig. 5. The radius of gyration, R_g, of the protein has been determined by linear least square fitting of the experimental R'_g versus concentration plot and extrapolation to zero concentration. This extrapolation eliminates concentration effects on R'_g values. The same procedure has been applied for determining the volume of the crotamine molecule: the apparent volume V' was obtained, from the ratio between $I(0)$ and the integral $Q = \int_0^\infty I(s)\, s^2\, ds$, for each concentration as described by Porod (1982):

$$V' = \frac{I(0)}{4\pi Q} \tag{2}$$

A linear extrapolation to zero concentration yielded the volume V of the molecule as shown in Fig. 5.

The molecular volume determined from the data of Fig. 5 is larger than that expected for a protein of molecular weight 4,870. This discrepancy may partially be explained by possible contributions of layer hydration effects, by errors involved in the determination of the $I(0)/Q$ ratio, and by uncertainties in the extrapolation procedure. Therefore we consider the volume V as a semiquantitative estimate. In further analysis this parameter is not used for quantitative purposes.

The surface area of the molecule was determined from the ratio between the limit value of $I(s)\, s^4$ versus s^4 for high s, and the integral Q (Pilz et al. 1979):

$$S = \frac{2\pi [I(s)\, s^4]}{Q} \tag{3}$$

Since SAXS intensities in the asymptotic region (high s value) present relatively large statistical errors and the concentration effect on SAXS intensities in this region is negligible, the surface area S of the molecule was determined as an average over the several surface areas obtained for different concentrations. All the structural parameters obtained are summarised in Table 1.

The wide domain of linear behavior of SAXS curves in Guinier plots suggests that the solution is monodisperse or that aggregation involves a very low fraction of molecules.

3.2. Determination of α-crotamine shape

The first and simplest assumption of a spherical molecular shape has been disregarded because the volume of a sphere calculated from the experimental radius of gyration $R_g = 13.7$ Å, $V_1 = 23.2 \times 10^3$ Å^3, is clearly different from the volume value calculated by using (2), $V_2 = 9.2\ 10^3$ A.

The second assumption was that of an ellipsoidal shape for the molecule, with semi-axes a, a, b. The plot of the volume of an ellipsoid with radius of gyration $R_g = 13.7$ Å versus the ratio of semi-axis $v = b/a$, shown in Fig. 6, suggests the possibility of either an oblate or a prolate ellipsoid, having a semi-axis ratio equal to 0.23 and 3.10, with surface areas of $3.2\ 10^3$ and $2.5\ 10^3$ Å^2, respectively. The surface area obtained using (3) is $S = (3.0 + 0.3)\ 10^3$ Å^2. This value is closer to

the surface area expected for an oblate ellipsoid but the high uncertainty associated with the value of S does not permit a clear conclusion. Therefore, we tried an alternative analysis of the scattering curve by determining the distance distribution function $p(r)$ and comparing it with the $p(r)$ function calculated from a structural model for the protein.

With the purpose of building a model for the molecule, a statistical prediction of the secondary structure was attempted by the methods of Chou and Fasman (1978) and hydrophobicity profiles (Cid et al. 1982). Table 2 lists the two independent and the combined predictions for the secondary structure of α-crotamine. It is noticeable that there is excellent agreement between the results of this secondary structure prediction and the proposed secondary structure content suggested by Hampe et al. (1978) and Hampe and Goncalves (1976), based on O.R.D., as well as with the results of Kawano et al. (1982) using Raman spectroscopy analysis.

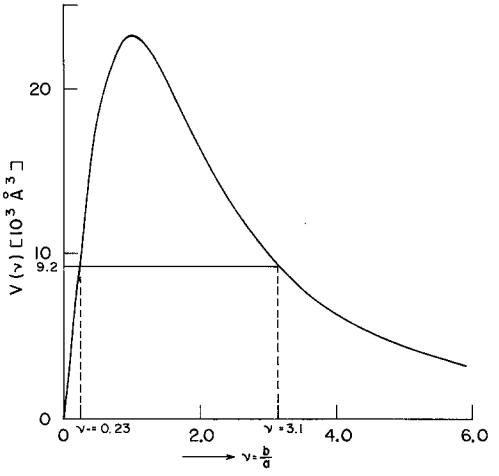

Fig. 6. Plot of the volume V of an ellipsoid with radius of gyration $R_g = 13.7$ Å versus the ratio of semi-axis. The intercept of this curve with the experimentally obtained volume gives the semi-axis ratio for a prolate and an oblate ellipsoid of that volume

A calculation of the distance distribution function, $p(r)$, was performed using desmeared intensity data, extrapolated to infinite dilution. The first quantitative information obtained from the experimental $p(r)$ function was the maximum diameter D of the particle. This parameter and its uncertainty have been determined by assuming decreasing values for D and introducing them in the ITP program for calculating $p(r)$. $D = (40 \pm 2)$ Å was found to be the minimum value which supresses oscillations of $p(r)$ close to $r \simeq D$.

We then tried to build a low resolution model for α-crotamine, based on the statistical prediction of the secondary structure, consisting of the association of two lobes linked by the disulphide bridge Cys18–Cys30. The larger lobe (L) includes residues from 1 to 17 and 31 to 42, while the smaller lobe (S) includes residues from 18 to 30. Lobe (L) is assumed to be a roughly symmetrically flattened spheroidal zone with a diameter of 22 Å and a height of 12 Å, while lobe (S) has a similar shape with a diameter of 18 Å and a height of 10 Å. Lobes (L) and (S) are interconnected by a neck of $4 \times 4 \times 1$ Å^3.

The Multibody program (Glatter 1980) was used for the calculation of $p(r)$ assuming a model with the geometry described above and filled with identical spherical scatterers with 1 Å radius. The theoretical $p(r)$ function calculated from this model, as well as the experimental $p(r)$ function obtained by Fourier transformation of the $sI(s)$ function, are shown in Fig. 7. The excellent agreement between the two curves indicates that the molecular model based on a two-lobe structure, derived from the statistical prediction, is fully compatible with the SAXS experimental results.

An analysis of the amino acid content of the two lobes of this α-crotamine model is presented in Table 3, showing that lobe (S) is considerably less polar than lobe (L). Although no mechanism of action is known for the toxic action of α-crotamine, this model suggests

Table 2. Prediction of the secondary structure for α-crotamine

Chou and Fasman		Hydrophobicity		Combined prediction	
AA sequence	Secondary structure	AA sequence	Secondary structure	AA sequence	Secondary structure
2–7	α-helix	1–8	α-helix	1–8	α-helix
8–11	β-turn	8–13	β-strand	9–12	random coil
12–16	β-turn	13–16	β-turn	13–16	β-turn
16–20	β-strand	16–20	β-strand	16–20	β-strand
20–24	β-turn	21–14	β-turn	21–24	β-turn
25–29	random coil	24–38	β-strand	25–36	β-strand
30–36	β-strand				
37–40	β-turn	38–41	β-turn	37–40	β-turn
41–42	random coil	42	random coil	41–42	random coil

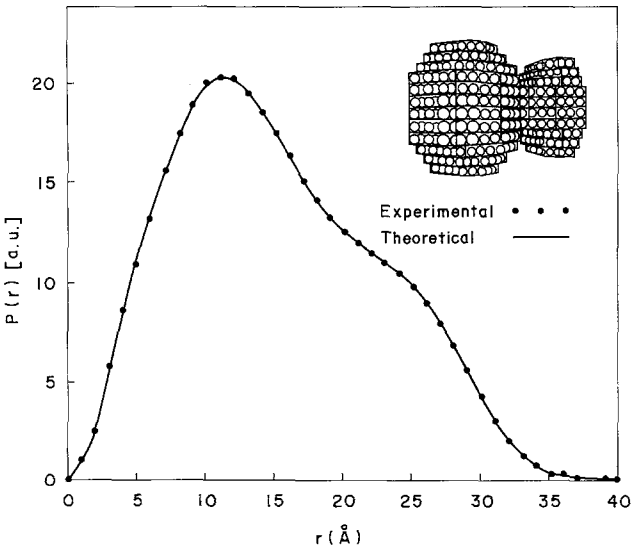

Fig. 7. Comparison between the $p(r)$ function determined from experimental SAXS results (in dots) and calculated for the (inserted) structural model of crotamine (continuous line)

Table 3. Nature of amino acids in crotamine and in each of lobes *L* and *S*

	α-Crotamine		Lobe *L*		Lobe *S*	
	number of a.a.	% a.a.	number of a.a.	% a.a.	number of a.a.	% a.a.
Non-polar a.a.	13	31	9	31	4	31
Uncharged polar a.a.	13	31	7	24	6	46
+Charged a.a.	13	31	12	41	1	8
−Charged a.a.	3	7	1	4	2	16

that, as lobe (*S*) is considerably less polar than lobe (*L*), it could play a role in the interaction of α-crotamine with cell membranes.

Acknowledgements. We are grateful to Dr. H. Cid who, during a visit to S. Carlos, did the secondary structure prediction of α-crotamine and to CNPq (Conselho Nacional de Desenvolvimento Cientifico), FAPESP (Fundacao de Amparo a Pesquisa do Estado de Sao Paulo) and FINEP (Financiadora de Projetos) for financial support.

References

Beltran JR, Mascarenhas YP, Craievich AF, Laure CJ (1985) SAXS study of structure and conformational changes of crotamine. Biophys J 47:33–35

Chou PY, Fasman GD (1977) β-turns in proteins. J Mol Biol 115:135–175

Chou PY, Fasman GD (1978) Empirical predictions of protein conformation. Ann Rev Biochem 47:251–276

Cid H, Bunster M, Arriagada E, Campos M (1982) Prediction of secondary structure of proteins by means of hydrophobicity profiles. FEBS Lett 150:247–254

Conti G, Laure CJ (1980) Pontes de dissulfeto da crotamina α. Annual Meeting of SBPC Abstract no 0.855

Glatter O (1980) Computation of distance distribution functions and scattering functions of models for small angle scattering experiments. Acta Phys Austr 52:243–256

Glatter O (1982) Practical aspects to the use of indirect Fourier transformations methods. Makromol Chem 183:465–479

Guinier A, Fournet G (1955) Small angle X-ray scattering. Wiley, New York

Hampe OG, Goncalves JM (1976) Optical rotatory dispersion of crotamine: effect of denaturants. Polymer 17:638–639

Hampe OG, Vozari-Hampe MN, Goncalves JM (1978) Crotamine conformation effect of pH and temperature. Toxicon 16:453–460

Kawano Y, Laure CJ, Giglio JR (1982) Laser Raman study on crotamine. Biochem Biophys Acta 705:20–25

Laure CJ (1975) Die Primostruktur des Crotamins. Hoppe-Seyter's Z Physiol Chem 356:213–215

Pilz I, Glatter O, Kratky O (1979) Small angle X-ray scattering. In: Hirs CHW, Timasheff SN (eds) Methods in enzymology. Academic Press, London, pp 148–249

Porod G (1982) General theory. In: Kratky O, Glatter O (eds) Small angle X-ray scattering. Academic Press, London